Received: 3 May 2022 | Accepted: 2 December 2022

DOI: 10.1002/pros.24473

ORIGINAL ARTICLE

The Prostate WILEY

Tempol differential effect on prostate cancer inflammation: In vitro and in vivo evaluation

Isabela Rossetto MD[1] | Felipe Santos MD[1] | Larissa Kido PhD[2] | Celina Lamas PhD[1] | Fábio Montico PhD[1] | Valéria Cagnon PhD[1]

[1]Department of Structural and Functional Biology, State University of Campinas (UNICAMP), Campinas, São Paulo, Brazil

[2]Department of Food and Nutrition, State University of Campinas (UNICAMP), Campinas, São Paulo, Brazil

Correspondence

Isabela, Rossetto, MD, Department of Structural and Functional Biology, State University of Campinas, 255 Monteiro Lobato St., Campinas, SP 13083-862, Brazil.
Email: isabela.urra.rossetto@gmail.com

Funding information

Fundação de Amparo à Pesquisa do Estado de São Paulo, Grant/Award Numbers: 2018/21647-6, 2021/02108-0; Conselho Nacional de Desenvolvimento Científico e Tecnológico, Grant/Award Number: 140699/2019-8

Abstract

Background: Tempol is a redox-cycling nitroxide that acts directly on inflammation. However, few studies have reported the use of tempol in prostate cancer (PCa). The present study investigated the effects of tempol on inflammation related to NF-κB signaling, using hormone-dependent or hormone-independent cell lines and the transgenic adenocarcinoma of the mouse prostate PCa animal model in the early and late stages of cancer progression.

Methods: PC-3 and LnCaP cells were exposed to different tempol doses in vitro, and cell viability assays were performed. The optimal treatment dose was chosen for subsequent analysis using western blotting. Five experimental groups were evaluated in vivo to test for tempol effects in the early (CT12 and TPL12 groups) and late stages (CT20, TPL20-I, and TLP20-II) of PCa development. The TPL groups were treated with 50 or 100 mg/kg tempol. All control groups received water as the vehicle. The ventral lobe of the prostate was collected and subjected to immunohistochemical and western blot analysis.

Results: Tempol treatment reduced cellular proliferation in vitro and improved prostatic morphology in vivo, thereby decreasing tumor progression. Tempol reduced inflammation in preclinical models, and downregulated the initial inflammatory signaling through toll-like receptors, not always mediated by the MyD88 pathway. In addition, it upregulated iκB-α and iκB -β levels, leading to a decrease in NF-κB, TNF-α, and other inflammatory markers. Tempol also influenced cell survival markers.

Conclusions: Tempol can be considered a beneficial therapy for PCa treatment owing to its anti-inflammatory and antiproliferative effects. Nevertheless, the action of tempol was different depending on the degree of the prostatic lesion in vivo and hormone reliance in vitro. This indicates that tempol plays a multifaceted role in the prostatic tissue environment.

KEYWORDS

inflammation, PC-3 and LNCaP, prostate cancer, Tempol, TRAMP

This work was performed at State University of Campinas (UNICAMP), at Institute of Biology (IB), Department of Structural and Functional Biology.

1 | INTRODUCTION

Prostate cancer (PCa) is the most common noncutaneous malignancy and the second most common cause of death among men in the United States and Brazil.[1,2] Several authors have focused on the role of inflammation in PCa development, based on the hypothesis that an inflammatory injury could prompt carcinogenesis.[3,4] Sustained inflammation generates a multitude of reactive nitrogen and oxygen species, cytokines, chemokines, and growth factors. The constant high levels of these factors potentially lead to uncontrolled cellular proliferation and enhanced genomic instability.[5] The NF-κB transcription factor is considered a master regulator of inflammation in cancer and is an important target in the control of disease progression.[6]

Tempol (4-hydroxy-TEMPO) is a redox-cycling nitroxide that participates in the metabolism of many reactive oxygen species (ROS) and is considered a potent antioxidant.[7] It is a low-toxicity ampholyte compound with a high capacity to permeate cell membranes, the gastrointestinal tract, or the blood-brain barrier.[8] A series of tempol functions have been reported in the literature, including preserving mitochondria against oxidative damage, improving tissue oxygenation,[9,10] playing a neuroprotective role,[11] protecting normal cells from radiation while maintaining radiation sensitivity of tumor cells,[12] and decreasing spontaneous tumor formation.[13] Tempol applications have been studied over the years in animal injuries associated with increased ROS production, including cancer.[7]

The antitumor and cancer-preventative activities of tempol have been reported to be related to tempol interactions with cancer chemotherapeutic agents. Ewees et al.[14] observed that tempol, used as an adjuvant treatment with cisplatin, reduced nephrotoxicity and showed a protective role in the kidney. Recently, Ye et al.[13] demonstrated the role of tempol in the suppression of proliferation of ovarian cancer cells and in glutamine metabolism, pointing to tempol as a therapeutic strategy in association with other anticancer drugs.

In addition, tempol seems to act directly on inflammatory processes, particularly on NF-κB modulation.[15] However, despite tempol application in cancer, few studies have reported its use in PCa, and none of these studies have described its effects on inflammation in PCa analyses.[16,17]

Among the experimental procedures for the study of PCa, PC-3, and LNCaP are the most common cell models used to understand prostate tumoral behavior, and evaluate androgen responsiveness to cancer.[18,19] Regarding in vivo studies, the transgenic adenocarcinoma of the mouse prostate (TRAMP) model is considered a good alternative for studying PCa progression and chemoprevention approaches, with well-established cancer stages from 8 to 30 weeks of age.[20–22]

The aim of this study was to investigate the effect of tempol on inflammatory markers related to NF-κB signaling, considering the differential responses of PCa cell lines with distinct androgen reliance, and the TRAMP model in the early and late stages of cancer progression. We also aimed to show the histopathological effect of tempol, focusing on prostate cell proliferation and tumor incidence.

2 | MATERIALS AND METHODS

2.1 | Cell culture and reagents

Human PCa cell lines PC-3 and LNCaP were obtained from American Type Culture Collection (ATCC) and Rio de Janeiro Cell Bank, respectively. Both cell lines were maintained in RPMI-1640 medium (Vitrocell) at 37°C with 5% CO_2, supplemented with 10% fetal bovine serum (Vitrocell) and 1% penicillin/streptomycin (Vitrocell). Tempol (4-hydroxy-TEMPO, 176141, Sigma Aldrich) was dissolved directly in the medium at different concentrations.

2.2 | Determination of cell viability

Cells (PC-3 1×10^4 cells; LNCaP 1.5×10^4) were plated in 96-well plate in triplicate. After 24 h of incubation, cells were treated with or without tempol diluted in the medium (0.5, 1, 2, 4, 8, and 10 mM) for 24, 48, and 72 h. At the end of the treatment, the cells were incubated with 80 µl of thiazolyl blue tetrazolium bromide (MTT; Sigma Aldrich, 5655) dye solution for 40 min. Then 80 µl of DMSO was added to each well to dissolve purple formazan crystals formed in viable cells. Optical density was measured at 570 nm in a spectrometer reader (Synergy ™ 2, BioTek® Instruments, Inc). In addition, a cell viability control experiment was performed using DHT (5α-androstan-17β-ol-3-one, Sigma Aldrich, A-8380) for LNCaP cell line. The 10 nM DHT concentration was included in the medium in association to tempol (see Supporting Information: Figure 4).

The IC50 was calculated based on the MTT data. For subsequent analyses, one dose was chosen according to two conditions: [1] the dose must have presented statistical significance by analysis of variance [ANOVA]-one-way test, post-Dunnet test; and [2] the dose must be lower than pointed in IC50. The lowest dose to meet both criteria in cell lines was found at 48 h of exposure to tempol, 1 mM for PC-3 and 2 mM for LNCaP (see Supporting Information: Figures 1 and 2). To explore the effects of the same dose on a longer exposure time, experiments. were also performed for 72 h of exposure.

2.3 | Animals and experimental procedures

Fifty male TRAMP mice (C57BL/6-Tg(TRAMP)8247Ng/J X FVB/NJ)F1/J) were obtained from the Multidisciplinary Center for Biological Investigation of the State University of Campinas (CEMIB/UNICAMP). The animals were divided into five experimental groups ($n = 10$) to evaluate the effects of tempol in the early (CT12 and TPL12 groups) and late-stage (CT20, TPL20-I and TLP20-II) of PCa development (Figure 1). TPL groups were treated with 50 or 100 mg/Kg of tempol (4-Hydroxy-TEMPO, 97%, Sigma-Aldrich—176141) diluted in water, five times a week, during 4 weeks. After that, the animals were euthanized and ventral prostate lobes were processed for subsequent analyses. The experiment was carried out in accordance to Ethics Committee in the Use of Animals (CEUA 5115-1/2019, 5115-1(A)–2020).

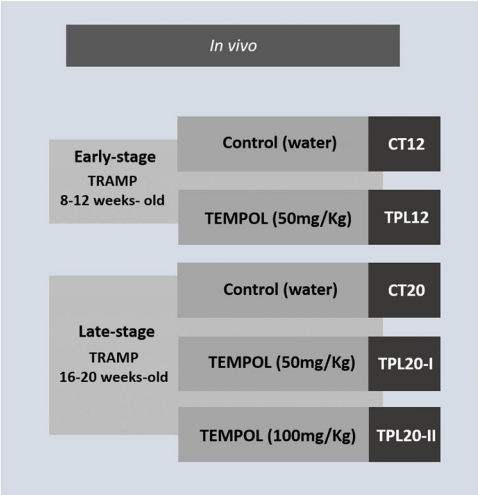

FIGURE 1 Experimental groups for in vivo tempol treatment according to prostate cancer progression

2.4 | Histopathological analysis

Five samples of ventral prostate lobe were collected from each experimental groups and fixed in Bouin's solution. The samples, washed in ethanol at 70%, passed through subsequent dehydration in an increasing series of alcohols. The fragments were cleared in xylene for 2 h and embedded in ultrafiltered paraffin plus plastic polymers (Paraplast Plus). Next, the prostate samples were sectioned using a Hyrax M60 microtome (Zeiss), into a thickness of 5 µm. Then, histological slides were stained in Hematoxylin-Eosin and photographed using a Nikon Eclipse E-400 photomicroscope (Nikon).

Histopathological analysis of the ventral prostate lobe was performed by capturing 10 random fields at ×400 magnification. The photomicrographs were divided into four quadrants. In each quadrant, prostate tissue was classified based on the morphological characteristics: Healthy epithelium (HE), Low Grade Prostatic Intraepithelial Neoplasia, High Grade Prostatic Intraepithelial Neoplasia, Well Differentiated Adenocarcinoma. Detailed classification criteria can be found in the Supporting Information: Table 1. The tissue morphological classification and lesion quantification were based on Berman-Booty et al.,[20] Gingrich et al.,[21] Kido et al.[23] and Da Silva et al.[24]

Animals that presented a palpable prostate tumor were counted and classified for analyses for Undifferentiated Adenocarcinoma (UA) incidence. The lobe-specific tumor incidence was confirmed by dissection during the euthanasia. These data were represented in tumor incidence percentage and then this distribution was evidenced in the each prostate lobe.

2.5 | Immunohistochemistry

Prostatic samples from the ventral lobe of 5 animals *per* group were collected and submitted to immunohistochemical analysis for PCNA, iNOS, COX-2, and IL-17 (for technical specifications, see Supporting Information: Table 2). The prostate samples were sectioned using a Hyrax M60 microtome (Zeiss) into a thickness of 5 µm, and collected in silanized slides. The antigen recovery was performed in citrate buffer (Ph 6.0) at 100°C in the microwave or treating with proteinase K, depending on the characteristics of the antibody. Blockade of endogenous peroxidases was obtained with H_2O_2 (0.3% in methanol) with subsequent blockage in bovine serum albumin (BSA) solution (3% in TBS-T), during 1 h at room temperature. The antibodies were diluted (1:35–500) in BSA 1% and applied in the tissue sections. The slides were storage overnight at 4°C. After TBS-T buffer washing, the sections were incubated with HRP conjugated secondary antibody from the Envision HRP kit (Dako Agilent) for 40 min and, later revealed with diaminobenzidine, according to manufacturer's instructions. The slides were counterstained with Harris' hematoxylin and analyzed using Nikon Eclipse E-400 photomicroscope (Nikon, ×40).

After immunostaining, 10 photomicrographs per animal per molecule were captured and a grid of 400 intersection points was superimposed on each photomicrograph. The grid intersections were considered positive points when located over a positive region for the analyzed molecule. To determine the intensity of immunostaining, the number of positive points was divided by the total number of grid points (400). The mean of each group was composed of the mean of the relative frequency of proliferating cell nuclear antigen (PCNA), iNOS, COX-2, and IL-17 for each animal.

2.6 | Western blot analysis

2.6.1 | Sample preparation

In vitro analysis: PC-3 (3×10^5) and LNCaP (4×10^5) cells were seeded in 60 mm^2 plates and allowed to attach overnight. Then, the plates were treated with or without tempol for each cell line. The samples were collected after 48 and 72 h of tempol treatment and processed for protein extraction. The experiment was performed with at least three passages of treated and properly processed PC-3 and LNCaP, being performed in technical and biological triplicate.

In vivo analysis: Prostatic samples (ventral lobe) were collected from five animals from each experimental group and processed for protein extraction.

2.6.2 | Protein extraction

In vivo and in vitro samples were lysed in nondenaturing extraction buffer (Lysis Buffer:NaCl 150 mM, Tris-HCl 50 Mm,1% Triton, 0,1% sodium dodecyl-sulfate [SDS], pH:8.00), plus 1% of aprotinin (A6279, Sigma-Aldrich). Then, the samples were homogenized using ultrasonic sonicator SONICS VibraCellsTM (Sonics & Material, Inc) and the tissue homogenate was centrifuged during 20 min at 15,000 rpm at 4°C. The protein quantification was measured by Bradford quantification method. Samples were mixed (1:1) with 2X sample buffer

Laemmli Sample Buffer (Bio-Rad Laboratories) plus 5% β-mercaptanol, incubated in a dry bath at 95°C for 5 min.

2.6.3 | Electrophoresis

Equal amounts of protein (50 µg) were blotted into 10%–12% SDS-PAGE gel and transferred onto nitrocellulose membranes (Hoefer System). Membranes were blocked in BSA 3% and the blots were incubated overnight with primary antibodies (for technical specifications, see Supporting Information: Table 2) and 2 h with a secondary antibody in the following day. The blot images were developed using a chemiluminescence kit (Super Signal West Pico Chemiluminescent/ Thermo Scientific/34080). The bands were visualized and captured by GeneGenome – Genesys system and chemicamera (Syngene). Pixels densitometry was calculated using the Uni-Scan-It 6.1 Program. β-actin was used as endogenous control for in vivo and in vitro analysis.

2.7 | Statistical analysis

In vitro analysis: Student's *t*-test was performed comparing control and treated groups for the chosen time points. ANOVA-one-way followed by Dunnett's test was carried out for cell viability assay.

In vivo analysis: the statistical analysis was considered separately for early-stage and late-stage groups. For the early-stage, Student's *t*-test was performed. For the late-stage, ANOVA-one-way was performed, followed by Tukey's test.

All data was previously considered parametric after Shapiro–Wilk's Test. The statistical analysis were perfomed using GraphPad Prism and with the level of significance set at 5% (version 7.00).

3 | RESULTS

3.1 | Decrease in cell viability in human PCa after tempol treatment

To determine the best experimental conditions, PC-3 (androgen-independent) and LNCaP (androgen-dependent) cell lines were exposed to different tempol concentrations for 24, 48, and 72 h. During the 24 h exposure, PC-3 cells showed lower sensitivity (IC_{50} = 6.3 mM) to tempol than LNCaP cells (IC_{50} = 4.2 mM). However, the PC-3 cells became more sensitive to tempol concentrations over time, leading to significant inhibition after 48 h (IC_{50} = 2.5 mM) and 72 h (1.9 mM) at 1.0 mM concentration (Figure 2A—see criteria for dose choice in Section 2 and Supporting Information: Material 2.1). In contrast, LNCaP presented a plateau behavior with similar responses during the 48 h (IC_{50} = 2.3 mM) and 72 h (IC_{50} = 2.2Mm) periods, leading to significant inhibition at 2.0 mM concentration (Figure 2B —see criteria for dose choice in Section 2 and Supporting Information: Material 2.1).

These results suggest that the efficacy of tempol may be related to the androgen responsiveness of human PCa cells. The LNCaP cell androgen dependence indicates early but sustained inhibition of viability caused by tempol throughout time. This result was confirmed based on the decrease in AR and PCNA protein levels with tempol in LNCaP cells at 48 and 72 h (Figure 2D). However, the lack of PC-3 androgen responsiveness suggests a time dependence of the tempol action. This result was confirmed by the decrease in PCNA in PC-3 after 1.0 mM treatment for 48 and 72 h (Figure 2C).

3.2 | Tempol modulated NF-κB signaling pathway in human PCa cells

The anti-inflammatory effect of tempol on PC-3 and LNCaP cells was evaluated, as different protein levels are related to the NF-κB pathway (Figure 3).

Two main mechanisms were observed in both cell lines after tempol exposure. The first mechanism involved downregulation of the initial inflammatory signaling through toll-like receptors. Tempol treatment showed no effect on TLR4 (Figure 3A,B), but decreased TLR2 levels after 48 and 72 h of exposure in both cell lines (Figure 3C,D). In addition, tempol downregulated MyD88, an important cytosolic adapter protein that plays a central role in the immune response (Figure 3E,F). The similar TLR4, TLR2, and MyD88 responses for LNCaP and PC-3 cell lines following tempol exposure suggest that tempol acts directly through the TLR-MyD88 pathway.

The second mechanism observed in both cell lines may be related to cytosolic NF-κB inhibition. Tempol upregulated iκB-α and iκB-β levels. IκB-α was upregulated after 48 h of tempol treatment in PC-3 and after 72 h in LNCaP cells (Figure 3G,H). IκB-β was particularly affected by tempol treatment, and was upregulated after 48 and 72 h in both cell lines (Figure 3I,J).

3.3 | Downregulation of NF-κB and other inflammatory marker levels after tempol exposure in human PCa cells

PC-3 cells showed a decrease in NF-κB total protein levels and TNF-α levels for all tempol treatment at different exposure times (Figure 4A,E). Effective downregulation of NF-κB after 72 h of tempol exposure was identified in LNCaP cells (Figure 4B). TNF-α inflammatory marker levels decreased in LNCaP cells after 48 and 72 h of exposure (Figure 4F).

3.4 | Possible interference of tempol in mechanisms related to cell death and survival in human PCa cell lines

The results showed that tempol interfered with cell death and survival markers. Tempol caused negative modulation of STAT-3,

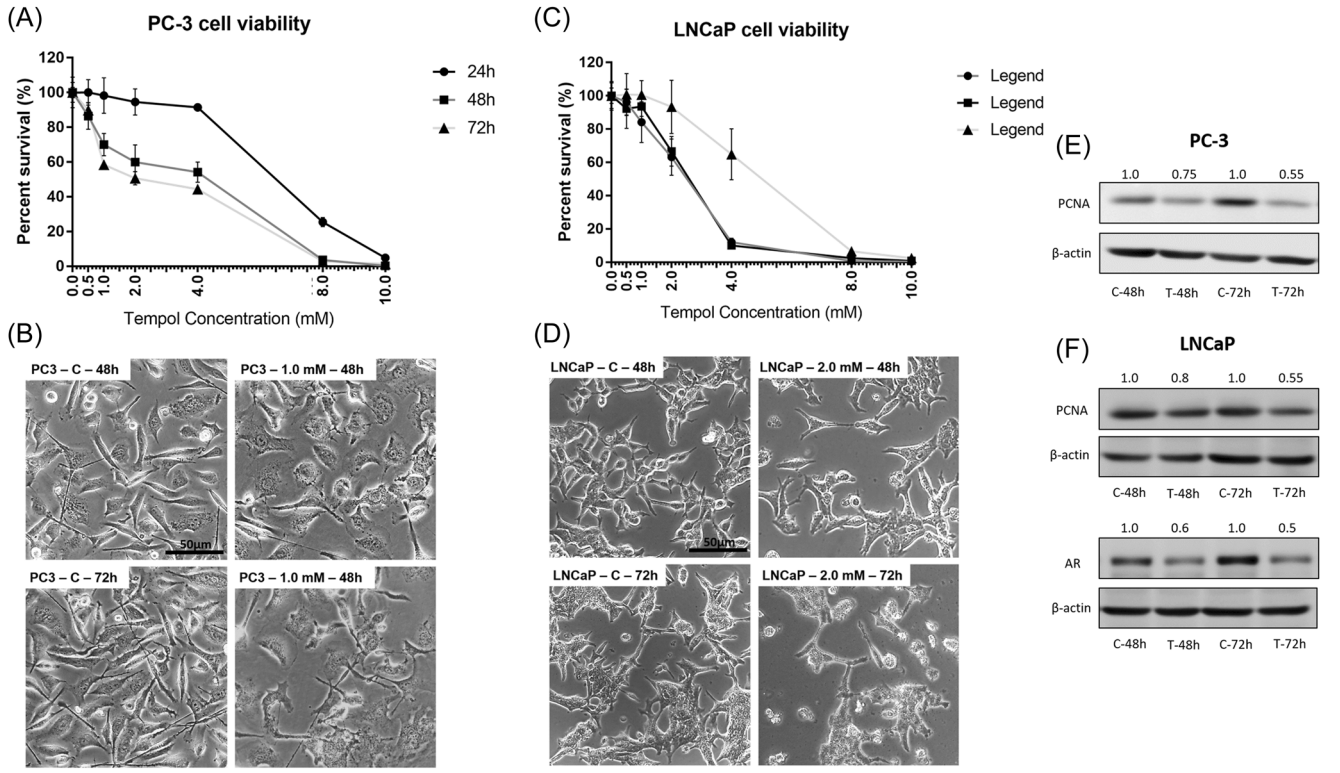

FIGURE 2 (A) Viability of the PC-3 cell line after 24, 48, and 72 h of exposition to different doses of tempol diluted in the medium. (B) Photomicrographs of the PC-3 Control and Tempol groups. (C) Viability of the LNCaP cell line after 24, 48, and 72 h of exposition to different doses of tempol diluted in the medium. (D) Photomicrographs of LNCaP Control and Tempol groups. (E) Representative Western blot bands demonstrating the effect of 1.0 mM of Tempol at 48 and 72 h on PC-3 cells. (F) Representative Western blot bands, demonstrating the effect of 2.0 mM of Tempol at 48 and 72 h on LNCaP cells. Numbers above the bands indicate fold-change of protein level when compared to the respective control group.

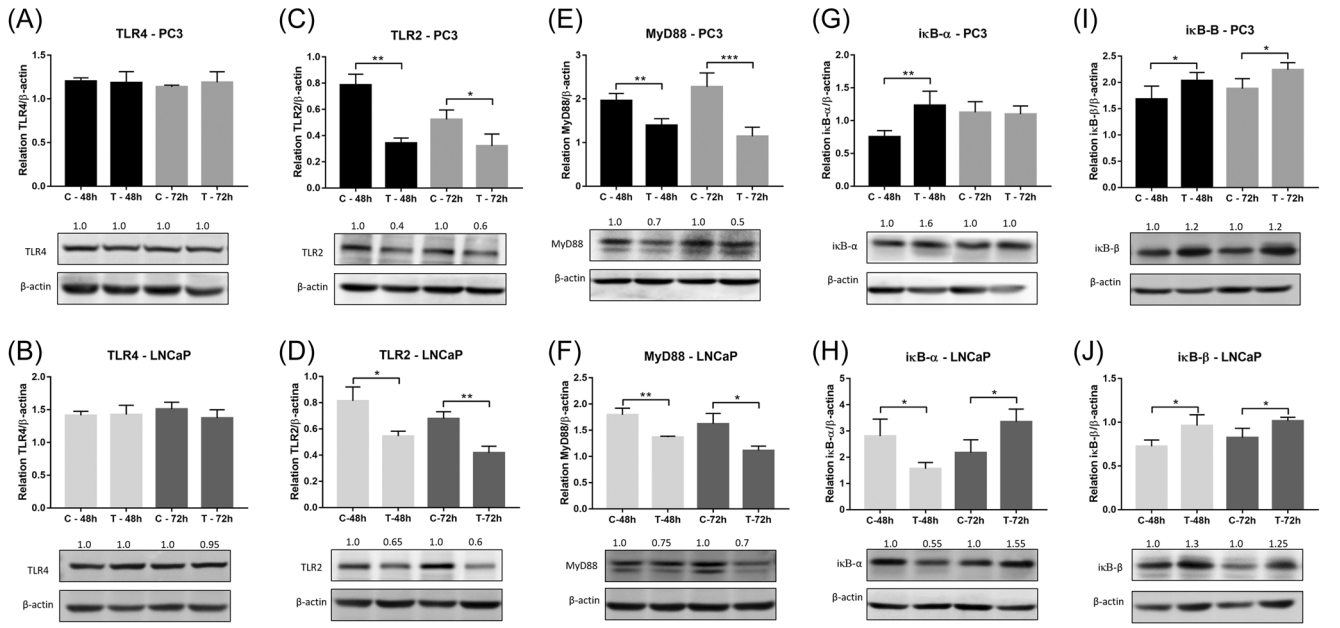

FIGURE 3 PC-3 and LNCaP protein levels after Tempol treatment, representative bands of protein blots and the respective fold-change related to control. Statistical significance was considered between the treated and nontreated group of the same time point (*$p < 0.05$; **$p < 0.01$; ***$p < 0.0001$).

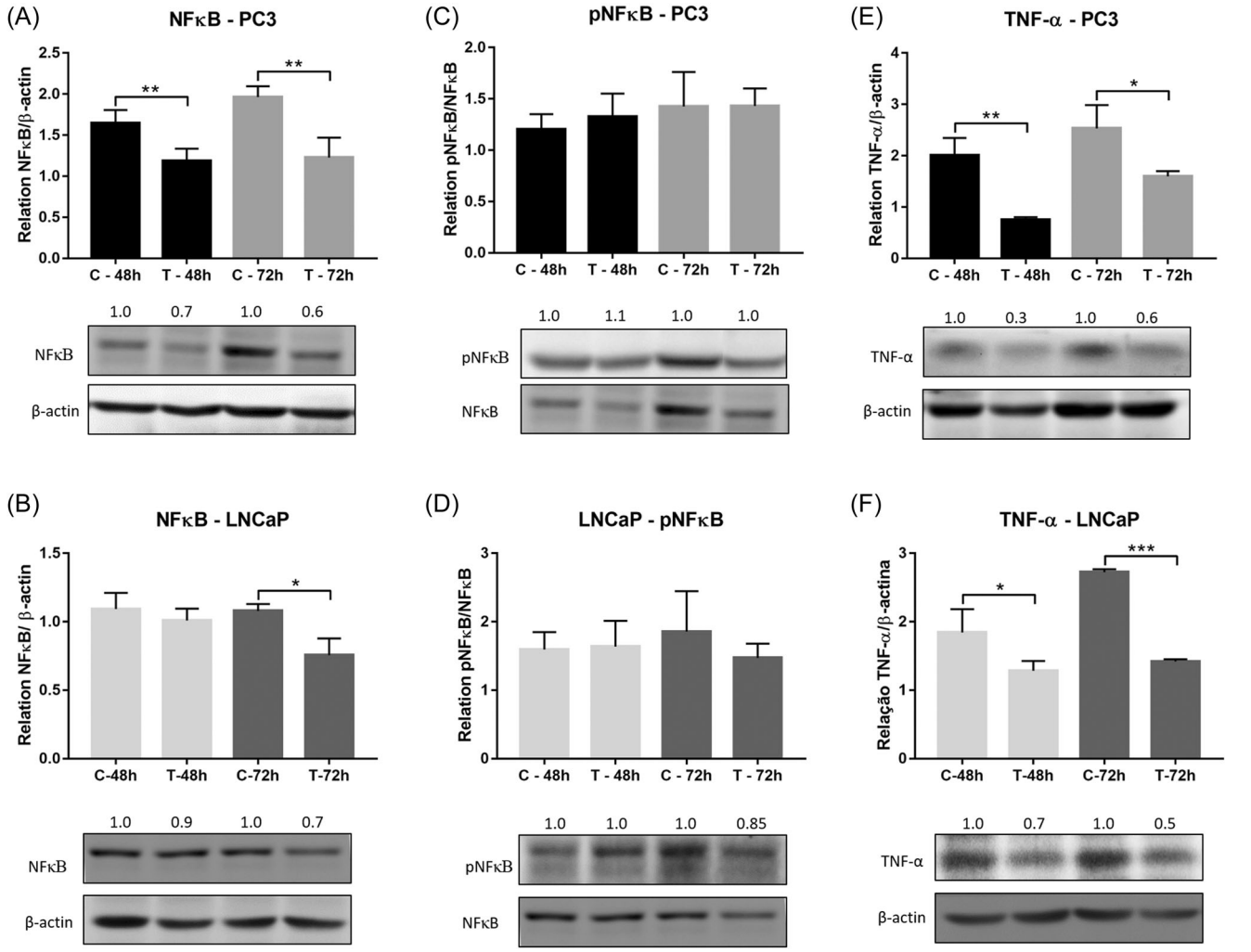

FIGURE 4 PC-3 and LNCaP protein levels after tempol treatment, representative bands of protein blots and the respective fold-change related to control. Statistical significance was considered between the treated and nontreated group of the same time point (*$p < 0.05$; **$p < 0.01$; ***$p < 0.0001$).

an important transcription factor related to the activation of inflammatory genes, in both cell lines for both treatment times (Figure 5A,B). In addition, tempol reduced BCL-2 antiapoptotic protein levels, mainly in the androgen-independent cell line PC-3 (Figure 5E). BCL-2 reduction occurred only after 72 h of tempol exposure in LNCaP androgen-dependent cells (Figure 5F). In contrast, tempol treatment did not affect the proapoptotic protein BAX (Figure 5G,H). A similar result was observed for caspase-3, which is related to cell death and was reduced after 48 h only in LNCaP cells (Figure 5J).

3.5 | Tempol reduced malignant lesion incidence changing PCNA and AR protein levels in vivo

In the TRAMP model, tempol treatment increased the frequency of HE in PCa early and late stages. Low-grade PIN was not altered in either stage, but the high-grade PIN incidence was significantly reduced in TPL12 and TPL20-I. The 100 mg/kg tempol dose in the TPL20-II group had no effect on high-grade PIN frequency. All treatments reduced the incidence of well-differentiated adenocarcinoma in the tempol groups compared to the respective control groups. Finally, we observed not only an improvement in the morphological parameters after tempol treatment, but also a reduction in PCNA epithelial immunolocalization (see Supporting Information: Material 2.2). In addition, AR protein levels decreased after tempol treatment in PCa early stages. In the late stage, we observed AR level reduction only in the TPL20-II group (Figures 6 and 7).

In the early stages, undifferentiated adenocarcinomas were not frequently observed. However, in the CT20 group, approximately 80% of the animals presented visible tumors. Results in the late stage showed a low incidence of undifferentiated adenocarcinomas in the TPL20-I and –II (Figure 7) after tempol treatment.

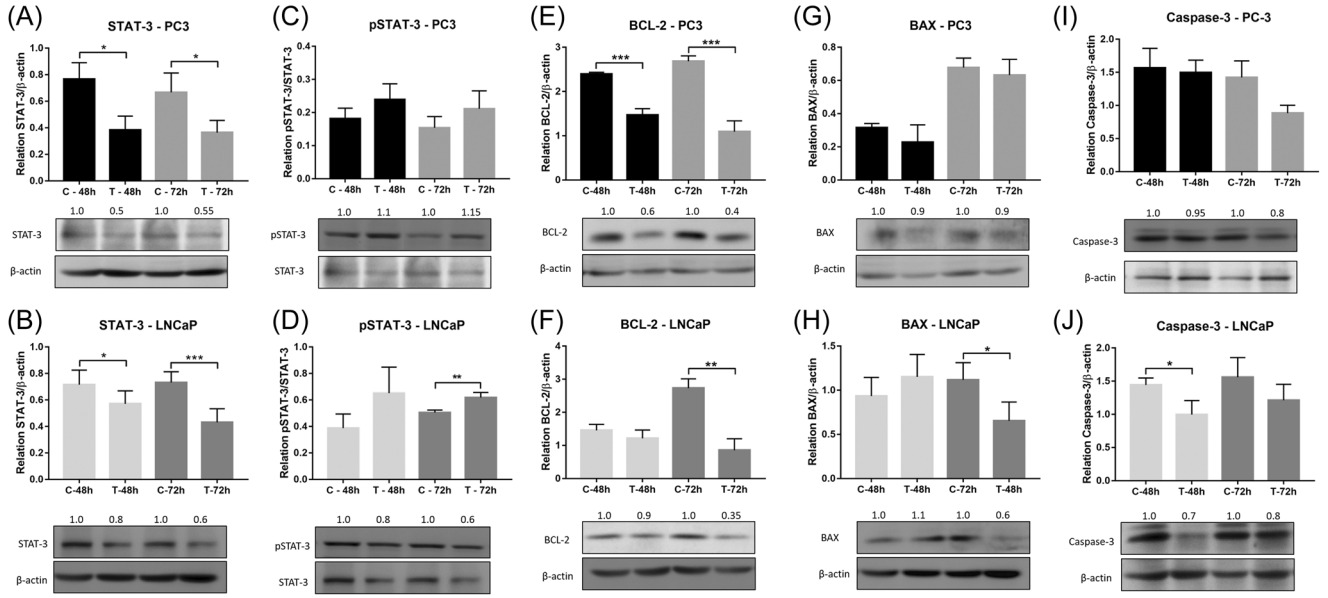

FIGURE 5 PC-3 and LNCaP protein levels after tempol treatment, representative bands of protein blots and the respective fold-change related to control. Statistical significance was considered between the treated and nontreated group of the same time point (*$p < 0.05$; **$p < 0.01$; ***$p < 0.0001$).

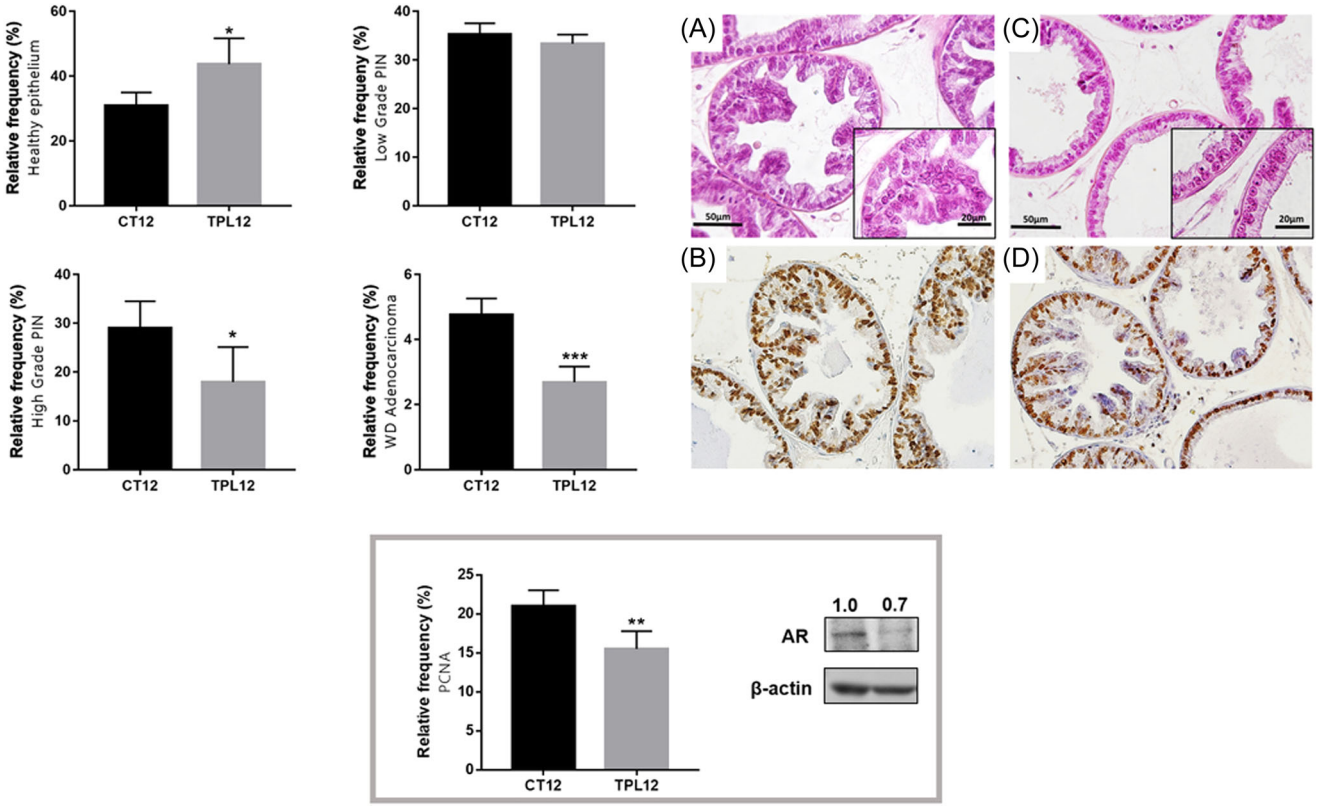

FIGURE 6 Morphological measurements for transgenic adenocarcinoma of the mouse prostate model in early-stage of cancer progression. On the right side, photomicrographs of main tissue findings in the CT12 (A) and TPL12 groups (C)—×40, hematoxilin and eosin—and PCNA immunostaining of the CT12 (B) and TPL12 groups (D)—×40, hematoxilin counterstaining. Under morphological results, graph of relative frequency of the PCNA immunostaining and Western blot analysis representative bands of the protein levels with respective fold-change related to control (*$p < 0.05$; **$p < 0.01$; ***$p < 0.0001$). [Color figure can be viewed at wileyonlinelibrary.com]

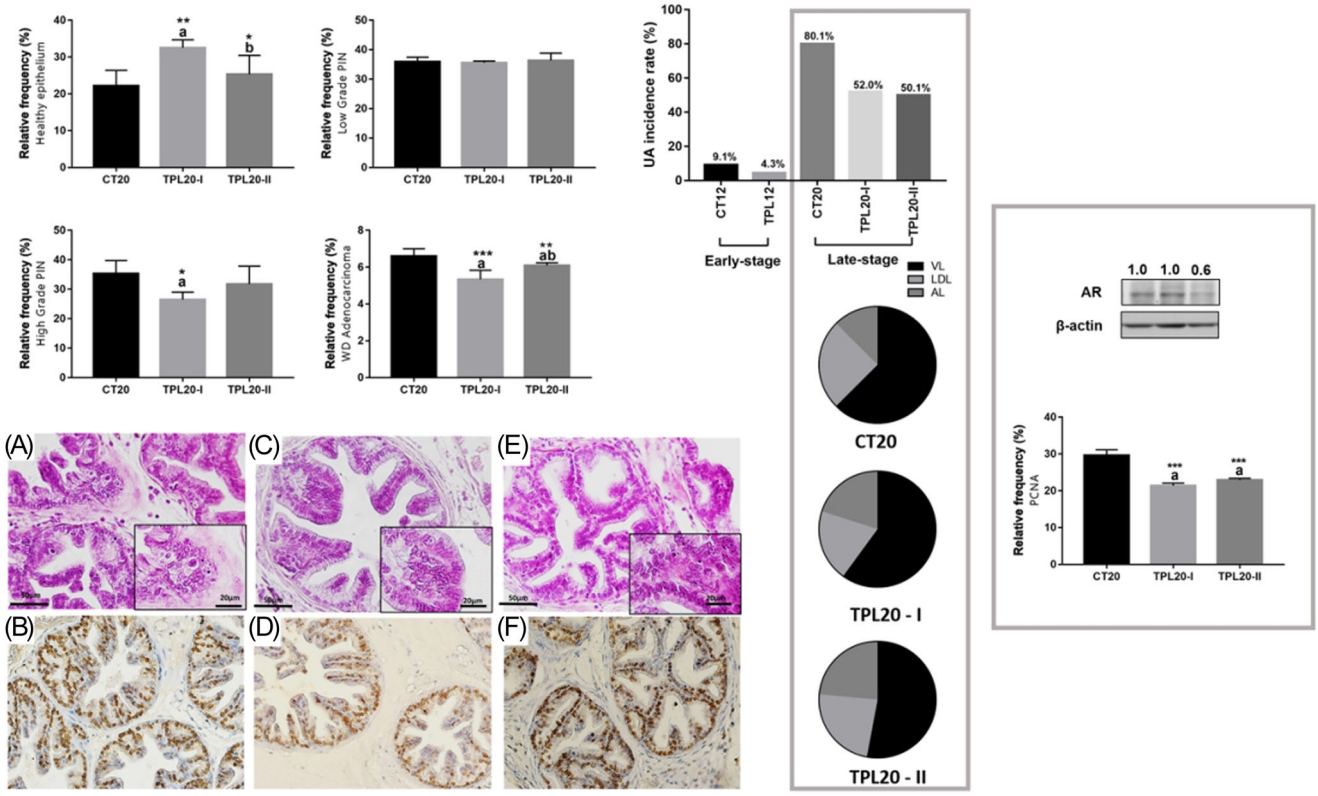

FIGURE 7 Morphological measurements for transgenic adenocarcinoma of the mouse prostate model in late-stage of cancer progression. Below the graphs, photomicrographs of main tissue findings of the CT20 (A), TPL20-I groups (C) and TPL20-II (E)—×40, hematoxilin and eosin—and PCNA immunostaining for CT20 (B), TPL20-I (D) and TPL20-II (F)— ×40, Hematoxilin counterstaining. On the right side, incidence rate of undifferentiated adenocarcinoma and distribution per lobe in late-stage of progression (AL, anterior lobe; LDL, dorsolateral lobe; VL, ventral lobe). In the right square, relative frequency for PCNA immunostaining and Western blot analysis representative bands for AR protein levels with respective fold-change related to control. For CT20, TPL20-I and TPL20-II, letter "a" denotes statistical significance when compared to CT20 group and letter "b" denotes statistical significance when compared to TPL20-I group (*$p < 0.05$; **$p < 0.01$; ***$p < 0.0001$). [Color figure can be viewed at wileyonlinelibrary.com]

3.6 | Tempol-mediated NF-κB modulation in cancer progression stages in vivo

Evaluation of the anti-inflammatory effects of tempol at different PCa stages showed important differential responses based on the cancer stage. Specifically, NF-κB signaling was modulated in vitro after exposure to tempol.

The mechanism of initial inflammatory signaling through toll-like receptors showed differential involvement of TLR4, TLR2, and MyD88 in the early and late stages of the treatment. In the early stages, TLR4 (Figure 8A) was not altered after treatment; however, tempol downregulated TLR2 levels (Figure 8C). At this stage, we observed an increase in MyD88 expression after exposure. At the same time, tempol decreased TLR4 and increased TLR2 levels at both treatment doses in the late stage (Figure 8B,D). MyD88 protein levels decreased with TPL20-I treatment and increased with TPL20-II treatment (Figure 8F). Thus, the MyD88 results suggest that the initial inflammatory signaling in vivo was not always MyD88-dependent.

The mechanism related to NF-κB cytosolic inhibition showed that iκB-β was particularly affected by tempol treatment, which was similar to the results observed for the cell lines (Figure 8I,J). IκB-α was downregulated in the early stage of treatment and upregulated in the late stage (Figure 8G,H).

3.7 | Tempol-mediated downregulation of inflammatory markers in vivo

NF-κB total protein levels were downregulated in the early stage after tempol treatment (Figure 9A). In the late stage, both doses decreased NF-κB levels, and pNF-κB levels increased with TPL20-II (Figure 9B,D). TNF-α, an important pro-inflammatory cytokine, decreased after tempol treatment with TPL12, TPL20-I, and–II (Figure 9E,F).

Other inflammatory markers were determined in the TRAMP model, and we observed a decrease in iNOS, COX-2, and IL-17 immunostaining during the early stage of treatment (Figure 9A–F).

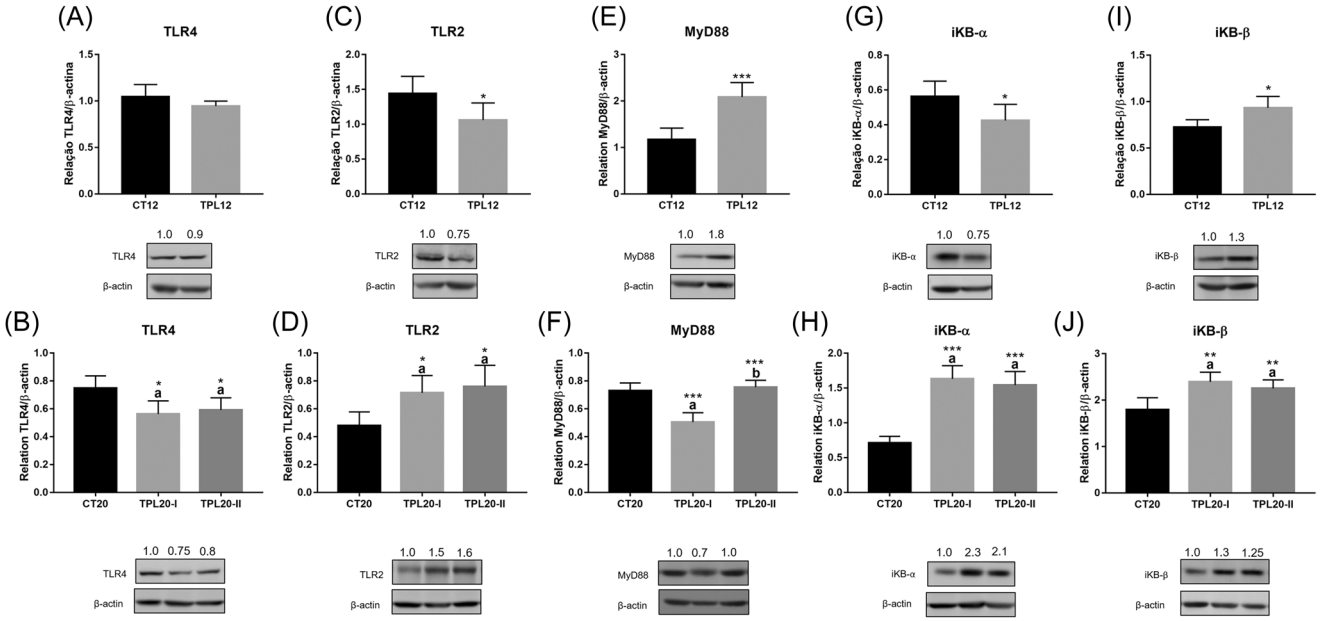

FIGURE 8 Transgenic adenocarcinoma of the mouse prostate model protein levels in early and late-stage of cancer progression, representative bands of protein blots and the respective fold-change related to control. For CT12 and TPL12, statistical significance was considered between the treated and nontreated group (*$p < 0.05$; **$p < 0.01$; ***$p < 0.0001$). For CT20, TPL20-I and TPL20-II, letter "a" denotes statistical significance when compared to CT20 group and letter "b" denotes statistical significance when compared to TPL20-I group (*$p < 0.05$; **$p < 0.01$; ***$p < 0.0001$).

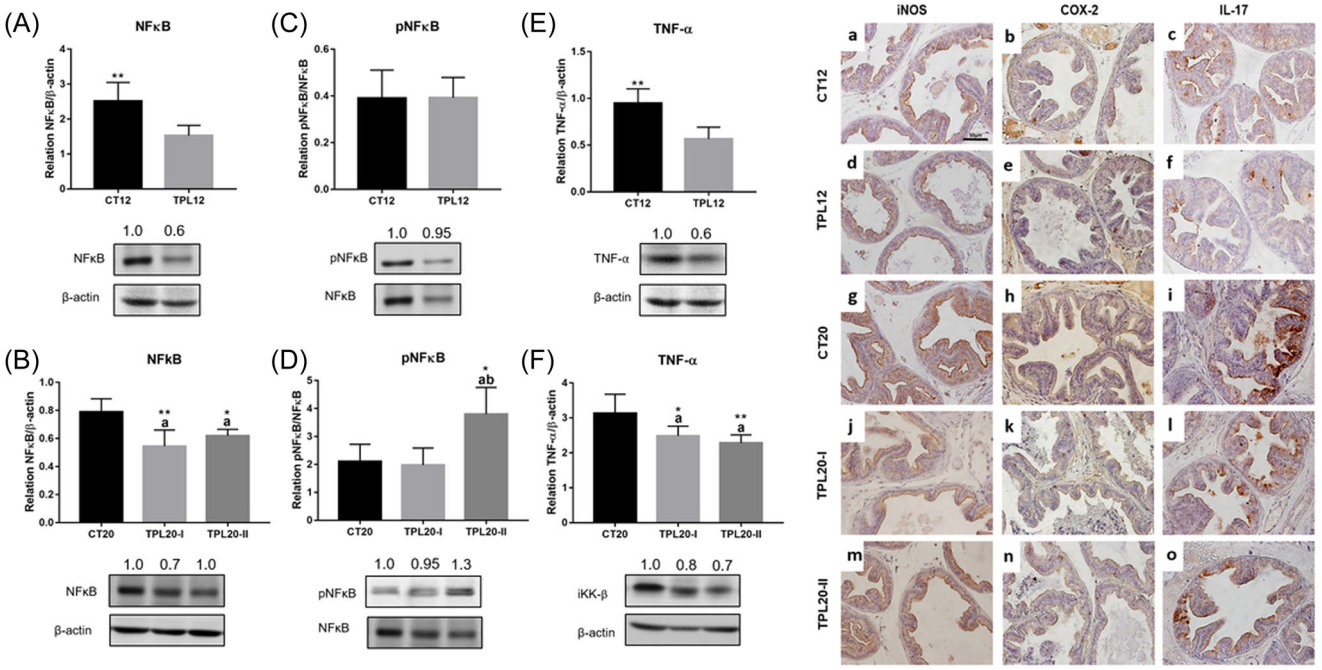

FIGURE 9 Transgenic adenocarcinoma of the mouse prostate model protein levels in early and late-stage of cancer progression, representative bands of protein blots and the respective fold-change related to control. For CT12 and TPL12, statistical significance was considered between the treated and nontreated group (*$p < 0.05$; **$p < 0.01$; ***$p < 0.0001$). For CT20, TPL20-I and TPL20-II, letter "a" denotes statistical significance when compared to CT20 group and letter "b" denotes statistical significance when compared to TPL20-I group (*$p < 0.05$; **$p < 0.01$; ***$p < 0.0001$). On the right side, photomicrographs of iNOS, COX-2, and IL-17 for each one of the groups (×40, hematoxylin counterstaining). [Color figure can be viewed at wileyonlinelibrary.com]

COX-2 and iNOS did not respond to tempol treatment during the late stage (Figure 9G–O). (See Supporting Information: Material 2.2).

3.8 | Tempol influenced cell death and survival in vivo

Tempol treatment altered STAT-3 and pSTAT-3 protein levels in the TRAMP model. In the early-stage, STAT-3 decreased in the TPL12 group (Figure 10A). In the late-stage, STAT-3 increased in the TPL20-II group and pSTAT-3 decreased in the TPL20-I and-II groups (Figure 10B,D).

We observed an increase in BCL-2, an antiapoptotic protein, associated with a decrease in BAX, a proapoptotic protein, in the early stage (Figure 10E,G). This tendency was very different from what was observed in the cell lines, suggesting an attempt towards tissue protection in this stage of cancer progression and a morphological dominance of healthy tissue in the TPL12 group. In the late stage, BCL-2 levels increased, and BAX levels decreased in the TPL20-II group (Figure 10F,H).

4 | DISCUSSION

The relationship between the inflammatory process and tempol application in PCa preclinical models is reported for the first time, showing the potential therapeutic role of tempol in inflammation. The results indicate molecular alterations in inflammatory signaling not only in vitro, in PC-3, and LNCaP tumor cells, but also in vivo, in the early and late stages of the TRAMP model cancer progression. Tempol treatment improved histopathological features of the prostate ventral lobe and delayed PCa evolution, protecting the tissue from the advance of cancer, particularly in the early stages.

Tempol is considered a nontoxic compound; however, there is no consensus on the dose and/or time for drug administration.[7] Some in vitro studies have evaluated different tempol doses ranging from 0.25 to 4 mM[16,17] on PCa cell lines; however, the correlation between dose and time of exposure was not evaluated. In this study, cell viability results showed that the sensitivity to tempol can be directly linked to the androgen independence or dependence of PC-3 and LNCaP cells. Thomas and Sharifi[17] determined that AR protein levels decreased in LNCaP cells after treatment with 2.5 mM tempol for 48 h, which was confirmed by the increased number of LNCaP cells in the sub G0 phase.

In agreement with the cell viability results, the histopathological improvement in the TRAMP ventral lobe in the early and late stages was associated with decreased AR and PCNA levels. The histological findings can be considered as a tempol dose reference and time administration guide for in vivo experiments, since this was the first time that tempol was tested on the TRAMP model. In vivo studies, which added tempol to water, were largely effective at 1–6 mM concentrations and showed no evidence of dose dependence in this concentration range.[7,8] In the present study, tempol's

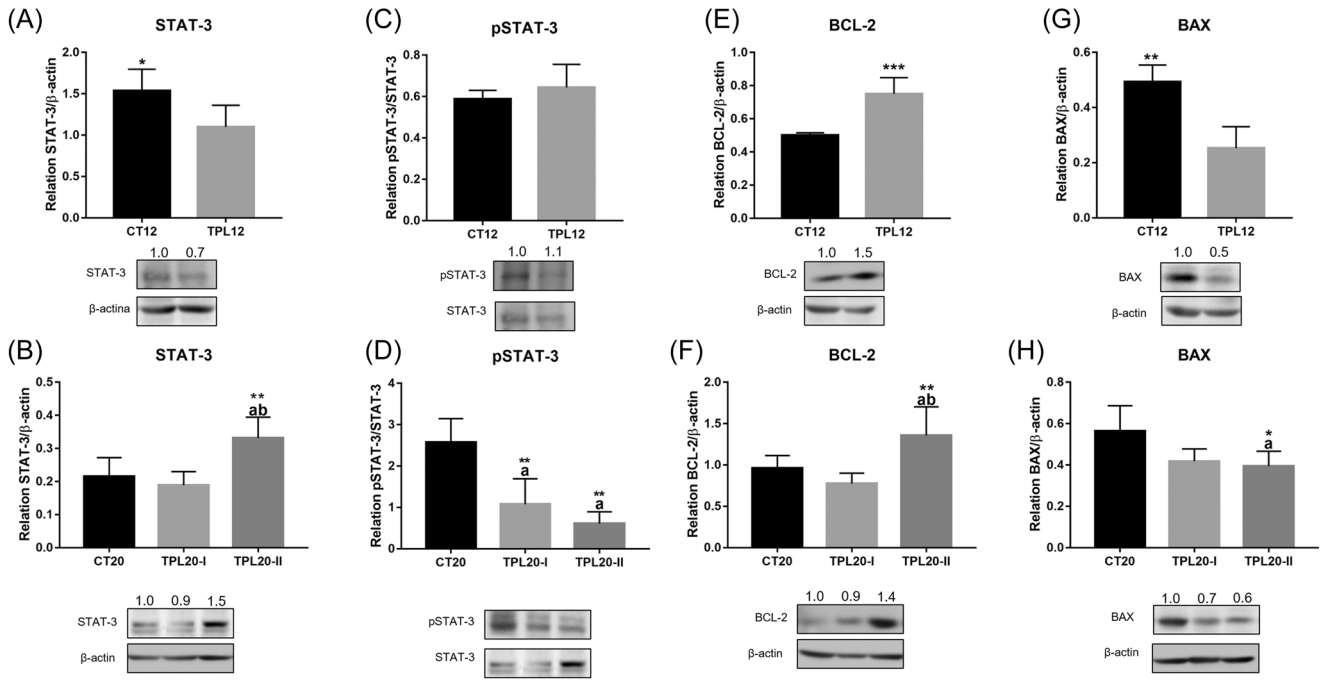

FIGURE 10 Transgenic adenocarcinoma of the mouse prostate model protein levels in early and late-stage of cancer progression, representative bands of protein blots and the respective fold-change related to control. For CT12 and TPL12, statistical significance was considered between the treated and nontreated group (*$p < 0.05$; **$p < 0.01$; ***$p < 0.0001$). For CT20, TPL20-I and TPL20-II, letter "a" denotes statistical significance when compared to CT20 group and letter "b" denotes statistical significance when compared to TPL20-I group (*$p < 0.05$; **$p < 0.01$; ***$p < 0.0001$).

dose-dependent effect on the TRAMP prostate was not clearly observed in the TPL20-II.

The relationship between tissue remodeling, proliferation signals, and inflammatory markers has already been established in the literature.[5] Therefore, the decrease in cell viability in vitro, prostate lesion, and tumor incidence in vivo can be considered positive signals of the anti-inflammatory role of tempol. Studies have shown that decreased cell proliferation is a strong signal of reduced NF-κB expression.[25] Androgen-independent cell lines, such as PC-3 and DU-145, have shown higher NF-κB levels than androgen-dependent cell lines, such as LNCaP and PNT1A, which have low basal NF-κB activation.[26,27] Shukla et al.[28] determined increased NF-κB expression during PCa progression in TRAMP model. In the present study, tempol treatment downregulated NF-κB levels in all experimental procedures studied. Based on this, we suggested a mechanistic hypothesis for the effect of tempol, indicating two distinct modulation points: (I) tempol led to a decrease or delay in the onset of the inflammatory cascade, and (II) tempol increased the NF-κB inhibitor levels in vitro and in vivo.

Regarding the ability of tempol to decrease or delay the onset of the inflammatory cascade, decreased TNF-α levels confirmed this hypothesis in in vitro and in vivo evaluations. Nonactivated NF-κB is located in the cell cytoplasm in association with proteins known as NF-κB inhibitors, such as iκBs.[29,30] NF-κB is then quickly recruited in response to a wide variety of stimuli, including pathogen signals, stress signals, and pro-inflammatory cytokines such as TNF-α and interleukins.[31] Similarly, TNF-α production is amplified by NF-κB activation, leading to an intensification of the inflammatory process due to the greater production of inflammatory cytokines in a positive feedback.[31] The reduction in TNF-α levels in all experimental procedures studied here emphasizes the potential of tempol as an eligible PCa therapy due to the suppressive effects on inflammation in the various pathways of this disease. Moreover, the decrease in NF-κB total protein levels also decreased the inflammatory cascade activation.

Decreased initial inflammatory signaling by tempol was confirmed by the differential modulation of toll-like receptors and MyD88. TLR4 and TLR2 have been widely investigated in the PCa microenvironment, and their expression is not restricted to immune cells, but also to healthy prostatic epithelial[32] and cancer cells.[33] TLR4 and TLR2 showed differential expression in LNCaP and PC-3 tumor cell lineages, and both of these receptors are linked to the MyD88 factor and NF-κB activity in the inflammatory pathway.[34] Based on the present results verified in tumoral cells PC-3 and LNCaP, tempol predominantly modulated TLR2 and MyD88, but did not involve TLR4. Literature has shown that the signaling pathway through TLRs, especially through TLR4, can be regulated depending on MyD88 involvement.[35] The lower MyD88 levels found after tempol treatment, indicate that inflammation signaling may be modulated by tempol in the tumoral cells by means of a MyD88-dependent pathway. TLR4 activation, when dependent on the MyD88 coupler, leads to MyD88 activation, which recruits IRAK and TRAF6 mediators, and degrades iκK-β, uninhibiting NF-κB, and resulting in the production of pro-inflammatory cytokines.[35]

Considering the in vivo results of the present study, early stage treatment was characterized by increased MyD88 levels. Thus, it can be hypothesized that the effect of tempol does not always depend on MyD88 in the TRAMP model. This is probably due to a decrease in inflammatory signaling caused by lower TLR2 activation. In contrast, the TLR4 level decrease in the late-stage cancer group suggests a decrease in inflammatory signaling by means of the TLR4-MyD88-dependent pathway, demonstrating that the 50 mg/kg tempol dose was more efficient than the 100 mg/kg dose in decreasing MyD88.

In addition, tempol activated the NF-κB inhibitor family, pointing to another downstream mechanism for inflammatory markers. We evaluated iκB-α and iκB-β protein levels, which play an additional role in regulating NF-κB activity when they are degraded. IκB-α is responsible for rapid and transient NF-κB activation, which is then quickly degraded in response to extracellular signaling and is resynthesized soon after.[36] In turn, iκB-β regulates chronic and persistent NF-κB activation.[37] Tempol significantly increased the iκB-β levels, which were consistently upregulated in all experimental PCa methods in this study. Based on this fact, we can infer that tempol stimulates chronic and persistent NF-κB maintenance in the cytosol, and that one of the mechanisms is associated with an increase in iκB-β levels.

Tempol decreased other in vivo inflammatory markers, such as IL-17, COX-2, and iNOS, particularly in the early stage group, which is known to be involved in the transition from prostatic intraepithelial neoplasms to well-differentiated or undifferentiated adenocarcinoma.[5,38] The present results indicate that tempol also interferes with cellular death and survival. BAX and BCL-2 are related to STAT-3 and are directly involved in apoptosis and programmed cell death, thereby maintaining the balance between healthy survival and tissue death.[39] The mechanism of increasing antiapoptotic proteins, such as BCL-2, or decreasing proapoptotic proteins, such as BAX, is an important mechanism by which tumor cells escape apoptosis.[10,39,40]

A significant tempol effect was observed in PC-3 and LNCaP cells, with decreased BCL-2 levels. However, the effects of tempol were not as evident for caspase-3 and proapoptotic BAX. The in vivo results suggest that tempol functions as a tissue protector, increasing BCL-2 and decreasing BAX in the early stage. Studies have pointed out that tempol is a tissue protector and an important drug in adjuvant therapies.[41] In addition, the morphological results confirmed the predominance of healthy tissue in the prostatic epithelium of TRAMP mice in the TPL12 group compared to that in the CT12 group. Ge et al.[41] showed that tempol led to the upregulation of BCL-2 and BAX decrease in an induced acute hepatotoxic model. In the late-stage group, tempol particularly interfered with the pSTAT-3 levels, decreasing the phosphorylation rate at both tempol treatment doses. This is an important finding, since STAT-3 is a transcription factor that regulates gene expression related to the cell cycle, cell survival, and immune response, and is associated with cancer progression and malignancy.[42] Based on these results, tempol did not seem to exert its effects on proapoptotic proteins in any experimental procedure considered. In contrast, it modulated STAT-3, which is essential for cell survival and is directly involved in NF-κB signaling.[43]

5 | CONCLUSION

This study identified that tempol affected the viability, proliferation, and survival of human PCa cell lines with distinct genetic backgrounds.

Tempol demonstrated chemopreventive activity, delayed PCa progression in the TRAMP model, and protected healthy prostate tissues. Furthermore, doubling the tempol dose in vivo did not maximize the effects of the lowest dose on the glandular response. Tempol was efficient in the inflammatory process, affecting toll-like receptors, activating or not the MyD88-dependent pathway, and increasing NF-κB inhibitors.

Finally, tempol can be considered a beneficial therapy for PCa treatment with anti-inflammatory and antiproliferative effects. Nevertheless, the effect of tempol was different depending on the degree of the prostatic lesion in vivo and hormone reliance in vitro. This indicates the multifaceted role of tempol in the prostatic tissue environment. Thus, further research will be useful to obtain more details about the effect of tempol in PCa angiogenesis, oxidative stress, and matrix remodeling.

ACKNOWLEDGMENT

This study was financed by São Paulo Research Foundation—FAPESP (grants: 2018/21647-6; 2021/02108-0) and in part by the National Council for Scientific and Technological Development (CNPq—grant: 140699/2019-8).

CONFLICT OF INTEREST

The authors declare no conflict of interest.

DATA AVAILABILITY STATEMENT

The data that support the findings of this study are available on request from the corresponding author. The data are not publicly available due to privacy or ethical restrictions.

ORCID

Isabela Rossetto http://orcid.org/0000-0002-4286-921X
Larissa Kido http://orcid.org/0000-0002-3653-8035
Fábio Montico http://orcid.org/0000-0001-8360-0842
Valéria Cagnon http://orcid.org/0000-0001-5331-7376

REFERENCES

1. Siegel RL, Miller KD, Fuchs HE, Jemal A. Cancer statistics: 2022. *CA Cancer J Clin*. 2022;72(1):7-33. doi:10.3322/caac.21708
2. Câncer de Próstata INCA. Disponível em. Accessed April 4, 2020. https://www.inca.gov.br/tipos-de-cancer/cancer-de-prostata
3. Cai T, Santi R, Tamanini I, et al. Current knowledge of the potential links between inflammation and prostate cancer. *Int J Mol Sci*. 2019;20(15):3833. doi:10.3390/ijms20153833
4. Falleiros-Júnior LR, Perez APS, Taboga SR, dos Santos FCA, Vilamaior PSL. Neonatal exposure to ethinylestradiol increases ventral prostate growth and promotes epithelial hyperplasia and inflammation in adult male gerbils. *Int J Exp Pathol*. 2016;97(5):380-388. doi:10.1111/iep.12208
5. Tewari AK, Stockert JA, Yadav SS, et al. Inflammation and prostate cancer. *Adv Exp Med Biol*. 2018;1095:41-65. doi:10.1007/978-3-319-95693-0_3
6. Nguyen DP, Li J, Yadav SS, Tewari AK. Recent insights into NF-κB signalling pathways and the link between inflammation and prostate cancer. *BJU Int*. 2014;114(2):168-176. doi:10.1111/bju.12488
7. Wilcox CS. Effects of tempol and redox-cycling nitroxides in models of oxidative stress. *Pharmacol Ther*. 2010;126(2):119-145.
8. Wilcox CS, Pearlman A. Chemistry and antihypertensive effects of tempol and other nitroxides. *Pharmacol Rev*. 2008;60:418-469.
9. Ahmed LA, Shehata NI, Abdelkader NF, Khattab MM. Tempol, a superoxide dismutase mimetic agent, ameliorates cisplatin-induced nephrotoxicity through alleviation of mitochondrial dysfunction in mice. *PLoS One*. 2014;9(10):e108889. doi:10.1371/journal.pone.0108889
10. Silva HNM, Covatti C, Rocha GL, et al. Oxidative stress, inflammation, and activators of mitochondrial biogenesis: tempol targets in the diaphragm muscle of exercise trained—mdx mice. *Front Physiol*. 2021;12:649793. doi:10.3389/fphys.2021.649793
11. Spejo AB, Teles CB, Zuccoli GS, Oliveira ALR. Synapse preservation and decreased glial reactions following ventral root crush (VRC) and treatment with 4-hydroxy-tempo (TEMPOL). *J Neurosci Res*. 2019;97(4):520-534. doi:10.1002/jnr.24365
12. Soule B, Hyodo F, Matsumoto K, et al. The chemistry and biology of nitroxide compounds. *Free Radic Biol Med*. 2007;42(11):1632-1650. doi:10.1016/j.freeradbiomed.2007.02.030
13. Ye S, Xu P, Huang M, et al. The heterocyclic compound tempol inhibits the growth of cancer cells by interfering with glutamine metabolism. *Cell Death Dis*. 2020;11:312. doi:10.1038/s41419-020-2499-8
14. Ewees MG, Messiha BAS, Abdel-Bakky MS, Bayoumi AMA, Abo-Saif AA. Tempol, a superoxide dismutase mimetic agent, reduces cisplatin-induced nephrotoxicity in rats. *Drug Chem Toxicol*. 2018;42(6):657-664. doi:10.1080/01480545.2018.1485688
15. Cuzzocrea S, Pisano B, Dugo L, et al. Tempol reduces the activation of nuclear factor-κB in acute inflammation. *Free Radic Res*. 2004;38(8):813-819. doi:10.1080/10715760410001710829
16. Lejeune D, Hasanuzzaman M, Pitcock A, Francis J, Sehgal I. The superoxide scavenger TEMPOL induces urokinase receptor (uPAR) expression in human prostate cancer cells. *Mol Cancer*. 2006;6(5):21. doi:10.1186/1476-4598-5-21
17. Thomas R, Sharifi N. SOD mimetics: a novel class of androgen receptor inhibitors that suppresses castration-resistant growth of prostate cancer. *Mol. Cancer Ther*. 2012;11:87-97.
18. Namekawa T, Ikeda K, Horie-Inoue K, Inoue S. Application of prostate cancer models for preclinical study: advantages and limitations of cell lines, patient-derived xenografts, and three-dimensional culture of patient-derived cells. *Cells*. 2019;8(1):74. doi:10.3390/cells8010074
19. Sanmukh SG, Dos Santos NJ, Barquilha CN, et al. Bacteriophages M13 and T4 increase the expression of anchorage-dependent survival pathway genes and down regulate androgen receptor expression in LNCaP prostate cell line. *Viruses*. 2021;13(9):1754. doi:10.3390/v13091754
20. Berman-Booty LD, Sargeant AM, Rosol TJ, et al. A review of the existing grading schemes and a proposal for a modified grading scheme for prostatic lesions in TRAMP mice. *Toxicol Pathol*. 2012;40(1):5-17. doi:10.1177/0192623311425062
21. Gingrich J, Barrios R, Foster B, Greenberg N. Pathologic progression of autochthonous prostate cancer in the TRAMP model. *Prostate Cancer Prostatic Dis*. 1999;2(2):70-75. doi:10.1038/sj.pcan.4500296
22. Kido LA, de Almeida Lamas C, Maróstica MR, Cagnon VHA. Transgenic Adenocarcinoma of the Mouse Prostate (TRAMP) model: a good alternative to study PCa progression and chemoprevention

approaches. *Life Sci*. 2019;217:141-147. doi:10.1016/j.lfs.2018.12.002
23. Kido LA, Montico F, Sauce R, et al. Anti-inflammatory therapies in TRAMP mice: delay in PCa progression. *Endocr Relat Cancer*. 2016;23(4):235-250. doi:10.1530/ERC-15-0540
24. Da Silva RF, Nogueira-Pangrazi E, Kido LA, et al. Nintedanib antiangiogenic inhibitor effectiveness in delaying adenocarcinoma progression in transgenic adenocarcinoma of the mouse prostate (TRAMP). *J Biomed Sci*. 2017;24(1):31. doi:10.1186/s12929-017-0334-z
25. Durand JK, Baldwin AS. Targeting iKK and NFkB for therapy. *Adv Protein Chem Struct Biol*. 2017;107:77-115. doi:10.1016/bs.apcsb.2016.11.006
26. Palayoor ST, Youmell MY, Calderwood SK, Coleman CN, Price BD. Constitutive activation of IκB kinase α and NF-κB in prostate cancer cells is inhibited by ibuprofen. *Oncogene*. 1999;18(51):7389-7394. doi:10.1038/sj.onc.1203160
27. Gasparian AV, Yao YJ, Kowalczyk D, et al. The role of IKK in constitutive activation of NF-κB transcription factor in prostate carcinoma cells. *J Cell Sci*. 2002;115:141-151. doi:10.1242/jcs.115.1.141
28. Shukla S, Maclennan GT, Marengo SR, Resnick MI, Gupta S. Constitutive activation of PI3K-Akt and NF-κB during prostate cancer progression in autochthonous transgenic mouse model. *Prostate*. 2005;64:224-239. doi:10.1002/pros.20217
29. Ghosh S, May MJ, Kopp EB. NF-κB AND REL PROTEINS: evolutionarily conserved mediators of immune responses. *Annu Rev Immunol*. 1998;16:225-260. doi:10.1146/annurev.immunol.16.1.225
30. Li Q, Verma IM. NF-κB regulation in the immune system. *Nat Rev Immunol*. 2002;2(10):725-734. doi:10.1038/nri910
31. Kalliolias GD, Ivashkiv LB. TNF biology, pathogenic mechanisms and emerging therapeutic strategies. *Nat Rev Rheumatol*. 2016;12(1):49-62. doi:10.1038/nrrheum.2015.169
32. Takeda K, Kaisho T, Akira S. Toll-like receptors. *Annu Rev Immunol*. 2003;21:335-376. doi:10.1146/annurev.immunol.21.120601.141126
33. Menendez D, Shatz M, Azzam K, Garantziotis S, Fessler MB, Resnick MA. The Toll-like receptor gene family is integrated into human DNA damage and p53 networks. *PLoS Genet*. 2011;7(3):e1001360. doi:10.1371/journal.pgen.1001360
34. Ou T, Lilly M, Jiang W. The pathologic role of Toll-Like receptor 4 in prostate cancer. *Front Immunol*. 2018;9:1188. doi:10.3389/fimmu.2018.01188
35. Thompson JE, Phillips RJ, Erdjumentbromage H, Tempst P, Ghosh S. IκB-β regulates the persistent response in a biphasic activation of NF-κB. *Cell*. 1995;80(4):573-582. doi:10.1016/0092-8674(95)90511-1
36. Well R, Whiteside ST, Israel A. Control of NF-κB activity by the IκBβ inhibitor. *Immunobiol*. 1997;198:14-23.
37. Zhang Q, Liu S, Ge D, et al. Interleukin-17 promotes formation and growth of prostate adenocarcinoma in mouse models. *Cancer Res*. 2012;72(10):2589-2599. doi:10.1158/0008-5472.CAN-11-3795
38. Fan Y, Mao R, Yang J. NF-κB and STAT3 signaling pathways collaboratively link inflammation to cancer. *Protein Cell*. 2013;4(3):176-185. doi:10.1007/s13238-013-2084-3
39. Paul-Samojedny M, Kokocińska D, Samojedny A, et al. Expression of cell survival/death genes: Bcl-2 and Bax at the rate of colon cancer prognosis. *Biochim Biophys Acta*. 2005;1741:25-29. doi:10.1016/j.bbadis.2004.11.021
40. Abouzied MM, Eltahir HM, Taye A, Abdelrahman MS. Experimental evidence for the therapeutic potential of tempol in the treatment of acute liver injury. *Mol Cell Biochem*. 2016;411:107-115.
41. Ge Z, Wang C, Zhang J, Li X, Hu J. Tempol protects against acetaminophen induced acute hepatotoxicity by inhibiting oxidative stress and apoptosis. *Front Physiol*. 2019;10:660. doi:10.3389/fphys.2019.00660
42. Furtek SL, Backos DS, Matheson CJ, Reigan P. Strategies and approaches of targeting stat3 for cancer treatment. *ACS Chem Biol*. 2016;11(2):308-318. doi:10.1021/acschembio.5b00945
43. Shrihari T. Dual role of inflammatory mediators in cancer. *Ecancermedicalscience*. 2017;11:721. doi:10.3332/ecancer.2017.721

SUPPORTING INFORMATION

Additional supporting information can be found online in the Supporting Information section at the end of this article.

How to cite this article: Rossetto I, Santos F, Kido L, Lamas C, Montico F, Cagnon V. Tempol differential effect on prostate cancer inflammation: in vitro and in vivo evaluation. *Prostate*. 2022;1-13. doi:10.1002/pros.24473